Nuclear Engineering and Technology 51 (2019) 853–859

Contents lists available at ScienceDirect

Nuclear Engineering and Technology

journal homepage: www.elsevier.com/locate/net

Original Article

An extensive investigation on gamma ray shielding features of Pd/Ag-based alloys

O. Agar [a], M.I. Sayyed [b, *], F. Akman [c], H.O. Tekin [d, e], M.R. Kaçal [f]

[a] Karamanoğlu Mehmetbey University, Department of Physics, Karaman, Turkey
[b] University of Tabuk, Department of Physics, Faculty of Science, Tabuk, Saudi Arabia
[c] Bingöl University, Vocational School of Technical Sciences, Department of Electronic Communication Technology, 12000, Bingöl, Turkey
[d] Uskudar University, Vocational School of Health Services, Radiotherapy Department, Istanbul, 34672, Turkey
[e] Uskudar University, Medical Radiation Research Center, 34672, Istanbul, Turkey
[f] Giresun University, Arts and Sciences Faculty, Department of Physics, 28100, Giresun, Turkey

ARTICLE INFO

Article history:
Received 9 December 2018
Received in revised form
19 December 2018
Accepted 20 December 2018
Available online 21 December 2018

Keywords:
Alloys
Shielding material
MCNPX
Photon
HPGe detector

ABSTRACT

A comprehensive study of photon interaction features has been made for some alloys containing Pd and Ag content to evaluate its possible use as alternative gamma radiations shielding material. The mass attenuation coefficient (μ/ρ) of the present alloys was measured at various photon energies between 81 keV–1333 keV utilizing HPGe detector. The measured μ/ρ values were compared to those of theoretical and computational (MCNPX code) results. The results exhibited that the μ/ρ values of the studied alloys are in the same line with results of WinXCOM software and MCNPX code results at all energies. Moreover, Pd75/Ag25 alloy sample has the maximum radiation protection efficiency (about 53% at 81 keV) and lowest half value layer, which shows that Pd75/Ag25 has superior gamma radiation shielding performance among the other compared alloys.

1. Introduction

Shielding against high-energetic gamma photons is absolutely mandatory at reactor or nuclear research center in order to reduce the dose level up to allowable limits [1]. The type and thickness of the required shielding material are related to the types of radiation, activity of the radio-isotope, cost effectiveness and exposure rate. A forceful shield material leads to both a significant energy loss at a small penetration distance and reduces as much as possible the possibility of further emission of dangerous radiations [2]. Since traditional radiation shielding materials namely lead (Pb) and concretes have few disadvantages such as toxicity, strength, etc., many researchers reported some novel and alternative shielding materials such as glass, alloy and polymer to prevent from gamma radiation [3–8].

Among alternative materials, alloys have been paid attention to widely used in different fields such as transportations, aerospace, modern technologies, biomedical and pharmaceutical industries. Their main basic features are to provide better qualities than the parent elements by composing of two or more elements with different structures that can improve advanced properties namely hardness, corrosion resistance and tensile strength [9]. In recent years, there are a great number of theoretical and computational (based on different simulation codes) investigations on photon shielding efficiency of various alloy materials [3,10–14]. Singh and Badiger reported the gamma photons attenuation parameters of nine alloys such as cupero-nickel, monel-400, carbon-steel (CS)-516, stainless steel (SS)-403 and incoloy-600 [15] and found the cupero-nickel has superior gamma photon shielding in comparison with the other alloys. Chen et al. [16] surveyed both the shielding and mechanical performances for the Mg–Zn–xCu–Zr alloys (x = 0–2.32 wt%). They observed that shielding effectiveness was enhanced meaningfully with increment of Cu content and the sample containing 2.32 wt% Cu represented the optimal EMI shielding capacity. Recently, the gamma ray shielding parameters have been determined for the Al-based glassy alloys by Manjunatha et al. [17] and $Al_{60}Y_{33}Ni_5Co_1Fe_{0.5}Pd_{0.5}$ was found to be a suitable shielding material for the gamma rays. Besides, Akman et al. [9] made comparison study of the photon shielding features of various alloy materials, which is composed of Ag, Cu, Pd and Cr elements, by experimental, WinXCom and MCNPX code for several energies

* Corresponding author.
E-mail address: mabualssayed@ut.edu.sa (M.I. Sayyed).

https://doi.org/10.1016/j.net.2018.12.014

between of 81–1333 keV and found that the Ag92.5/Cu7.5 sample is the most effective shield material among the selected alloys.

On the other hand, silver-palladium alloys are of scientific interest and nowadays they are used in several applications such as electrical contact materials, in medical and dental fields [18]. The main aim of this study is to determine the gamma photon attenuation parameters of various alloys by doped in different rates of Pd and Ag for radiation detection applications. It has been measured the experimental mass attenuation coefficients at photon energies between 80.997 and 1332.501 keV using the transmission geometry technique. The mass attenuation coefficient (μ/ρ) values of the investigated alloys have been computed theoretically (WinXCom software) and also simulated by MCNPX code to test the confirmation of the experimental results.

2. Material and method

2.1. Theoretical basis

The linear attenuation coefficient of the samples under investigation is defined from the well-known exponential attenuation rule:

$$\mu = -\frac{\ln \frac{I}{I_0}}{x} \tag{1}$$

in the previous equation I and I_0 denote respectively the transmitted and initial intensities.

Since the alloy sample contains more than one element, the μ/ρ can be evaluated from the mixture rule namely [19]:

$$\frac{\mu}{\rho} = \sum w_i \left(\frac{\mu}{\rho}\right)_i \tag{2}$$

where w_i is the weight fraction of the ith element in the material. It is expressed in cm^2/g. The μ_m value of alloys can be calculated for a specific energy range using WinXCom software based on the mixture rule [20].

The molecular cross section can be computed utilizing the above μ/ρ quantity as below [21]:

$$\sigma_{t,m} = \frac{1}{N_A}\left(\frac{\mu}{\rho}\right)_{Alloy} \sum_i (n_i A_i) \tag{3}$$

where N_A is the Avogadro number, n_i and A_i represent the number of element and the atomic weight of the ith element in the material, respectively. The total atomic cross section (σ_a) can be determined as follow [22,23]:

$$\sigma_{t,a} = \sigma_{t,m} \Big/ \sum_i n_i \tag{4}$$

Additionally, the total electronic cross-section (σ_e) can be expressed mathematically as [24]:

$$\sigma_{t,el.} = \frac{1}{N}\sum_i \left(\frac{\mu}{\rho}\right)_i \frac{f_i A_i}{Z_i} \tag{5}$$

The above three quantities presented in equations (3)–(5) helped us to determine the effective atomic number (Z_{eff}) for the investigated sample according to equation (6) [22]:

$$Z_{eff} = \frac{\sigma_a}{\sigma_e} \tag{6}$$

The radiation protection efficiency (RPE) also another parameter gives an indication about the effectiveness of any absorber to shield the photons and determined from both the original photon beam which emitted from the radioactive point source and the attenuated beam (owing to the presence of any absorber located between the source and the detector) counted on the detector. The RPE values for the samples under investigation are estimated by the following equation [25,26]:

$$RPE = \left(1 - \frac{I}{I_0}\right) * 100 \tag{7}$$

The half value layer (HVL) is the thickness at which the intensity of the attenuated photon is 50% the intensity of the original photon and depends inversely on the μ namely [27]:

$$HVL = \frac{ln2}{\mu} \tag{8}$$

2.2. Experimental details

The selected alloy samples in this investigation contain two elements namely palladium (Pd, Z = 46) and silver (Ag, Z = 47). The four selected alloy samples containing different fractions of 77, 75, 30 and 70% for Pd and 23, 25, 70 and 30 for Ag, which is tagged as Pd77/Ag23, Pd75/Ag25, Pd30/Ag70 and Pd70/Ag30, respectively. In addition, the densities of alloys are 11.16, 11.7, 10.9 and 11.6 g/cm^3 for Pd77/Ag23, Pd75/Ag25, Pd30/Ag70 and Pd70/Ag30, respectively.

Gamma ray spectrometer equipped with High purity germanium (HPGe) detector was employed to count the high-energy photons intensities of 81, 122, 136, 161, 276, 303, 356, 384, 511, 662, 835, 1173, 1275 and 1333 keV by using various radioactive point sources. The HPGe detector has an active crystal length and diameter of 25 and 70 mm, respectively, and a resolutions of 0.380 keV at 5.9 keV, 0.585 keV at 122 keV and 1.8 keV at 1330 keV full width at half maximum (FWHM) and is kept at liquid nitrogen temperature (−196 °C) during the experiments. The energy calibration for spectrometer was applied with help of a mixed calibration source including ^{22}Na, ^{54}Mn, $^{57,60}Co$, ^{137}Cs, ^{133}Ba, ^{203}Hg and ^{241}Am. The schematic arrangement of the experimental system used is exhibited in Fig. 1 [28]. Each alloy material was located between the detector and the radioactive point source. After spectrum acquisitions, the analyzes were made through ORTEC Maestro software package program [29,30]. The net area was counted utilizing the Origin 7.5 software (demo) with least-squares fit method. Additionally, the experimental uncertainty of attenuation coefficient measurements was determined by the relation [31–33]:

$$\Delta\mu/\rho = \frac{1}{\rho x}\sqrt{\left(\frac{\Delta I}{I}\right)^2 + \left(\frac{\Delta I_0}{I_0}\right)^2 + \ln\left(\frac{\Delta I}{I}\right)^2 \left(\frac{\Delta \rho x}{\rho x}\right)^2} \tag{9}$$

where $\Delta\rho x$ denotes the uncertainty in the mass per unit area, ΔI and ΔI_0 are the uncertainties of I and I_0 intensities, respectively.

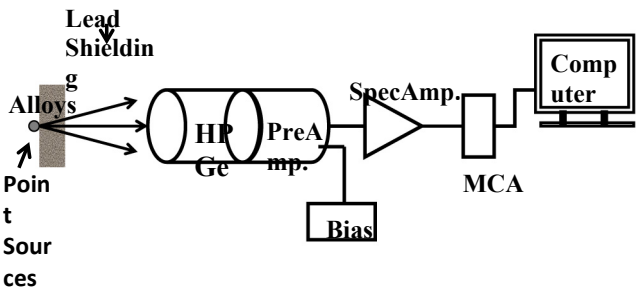

Fig. 1. Schematic layout of the experimental setup (revised from Ref. [28]).

2.3. MCNPX code

In order to assess the validity of the measured results, Monte Carlo N-Particle Transport Code System-extended (MCNPX) has been applied. Fig. 2 represents the MCNPX 3-D appearance of gamma photon attenuation layout with various simulation materials including a point radioactive source, the alloy as shielding material, Pb blocks to avoid the scattered photons, lead (Pb) collimator for primary radiation beam and F4 tally mesh detection field. The studied alloys have been located between the F4 tally mesh and the source at a distance of 50 cm. More details on simulation setup can be taken from our previous studies [34,35].

3. Results and discussion

The experimental μ/ρ results and their uncertainties calculated by detecting the intensity of photons that passes through the alloys have been demonstrated in Table 1. It can be easily seen from this table that these results of four alloy samples are decreased with increment of photon energy. Additionally, the uncertainties of μ/ρ values are in the range of 1.01%–4.61% for Pd77/Ag23 sample, 1.01–3.46% for Pd75/Ag25 sample, 1.00–4.72% and 1.01–4.84% for Pd70/Ag30 sample. The estimated uncertainty values can be ascribed to the counting statistics in intensities of original (I_0) and transmitted (I) photons, scattering effects and measurement of sample mass per unit area. These low uncertainties of μ/ρ demonstrate how the μ/ρ as well as other shielding parameters for the investigated alloy samples are measured with the high accuracy.

Moreover, the μ/ρ of the selected alloys has been calculated through both theoretical and computational techniques to validate the experimental data. Thence, the experimental μ/ρ results have been compared to values obtained by utilizing WinXCom software and MCNPX simulation code and represented graphically in Fig. 3. It is evident in Fig. 3 that the measured, WinXCom and MCNPX μ/ρ values of different alloys agreed quite well with each other. The percentage relative deviations (RD) among the experimental, WinXCom and MCNPX results of μ/ρ were established with the help of the following relations [36,37]:

$$RD = \left(\frac{\mu/\rho_{exp.} - \mu/\rho_{a,b}}{\mu/\rho_{exp.}}\right)*100 \quad (10)$$

where μ/ρ_a and μ/ρ_b denote the theoretical and computational μ/ρ values of the alloys.

The obtained RD values among results of different techniques were given in Fig. 4 and found in the range of −4.94–0.0% and −5.50–1.19% for experimental–WinXCom and experimental–MCNPX results of alloys samples, respectively. These differences can be based on the mixture rule that ignores the interactions between atoms in mixtures or compounds. Therefore, it can say that the measured μ/ρ data are in an agreement with both the theoretical and computational results.

Moreover, the μ/ρ value for the alloys reduces exponentially over the low energy region (up to about 400 keV) as the change in μ/ρ values is getting smaller with increasing of energy (E > 400 keV). The most important reason of this trend is due to several photon interaction processes. Briefly, the photoelectric absorption (PE) is the most important photon-matter interaction mode for E < 400 keV, while for 400 keV < E < 1330 KeV Compton scattering (CS) processes is more dominant than PE. The PE and CS processes are depending upon the energy as $E^{-3.5}$ and E^{-1} respectively. This demonstrates the quick reducing happens for the μ/ρ for energy less than 400 keV. It is worth mention that all samples have the highest attenuation value at the lowest energy (i.e. at 81 keV), this is owing to the dependence of PE on the atomic number as Z^{4-5}. While with further increase in the energy, the μ/ρ for the four samples become very close to each other. This is maybe due to the dependence of CS on the atomic number, where this process is proportional to the atomic number as Z.

Additionally, the results revealed that the μ/ρ values have the descending order of Ag70/Pd30 (2.4020 ± 0.0241 cm^2/g) > Pd70/Ag30 (2.3888 ± 0.0241 cm^2/g)> Pd75/Ag25 (2.3569 ± 0.0237 cm^2/g) > Pd77/Ag23 (2.3342 ± 0.0235 cm^2/g) at 81 keV energy (see Table 1). It means that Ag70/Pd30 alloy sample has the maximum mass attenuation coefficient among the investigated alloy samples. This is due to fact that Ag70/Pd30 has a content of higher atomic number (i.e Ag) with fraction of 70%.

Another parameter is the radiation protection efficiency (RPE) obtained from the intensities of original (I_0) and transmitted (I) photon intensity as given in Equation (7). This parameter plays an important role in comparison of the performances of the selected samples to attenuate the incoming photons. Fig. 5 indicates the variation of the RPE for the studied alloy samples. From Fig. 5, all the RPE values were reduced depending on increment of the photon energy. Among alloys in this study, Pd75/Ag25 sample has the maximum RPE (about 53% at 81 keV). This result implies that

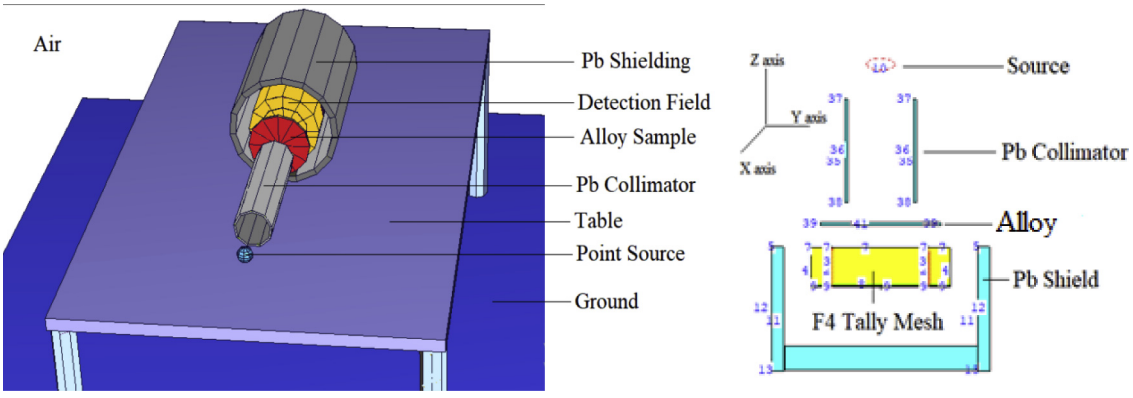

Fig. 2. **(a)** 3-D MCNPX setup obtained from MCNPX Visualization Editor *(VE_VersionX_22S)* and **(b)** a general-view of designed simulation setup.

Table 1
The experimental mass attenuation coefficients (cm^2/g) results of the investigated alloys.

Energy (keV)	Pd77/Ag23		Pd75/Ag25		Ag70/Pd30		Pd70/Ag30	
	Exp.	Error	Exp.	Error	Exp.	Error	Exp.	Error
81	2.3342	0.0235	2.3569	0.0237	2.4020	0.0241	2.3888	0.0241
122	0.8059	0.0088	0.8251	0.0090	0.8340	0.0099	0.8086	0.0099
136	0.6292	0.0179	0.6375	0.0157	0.6514	0.0294	0.6212	0.0189
161	0.4249	0.0196	0.4360	0.0151	0.4511	0.0202	0.4352	0.0206
276	0.1636	0.0045	0.1646	0.0042	0.1506	0.0066	0.1628	0.0066
303	0.1459	0.0041	0.1479	0.0040	0.1481	0.0070	0.1440	0.0060
356	0.1196	0.0041	0.1197	0.0037	0.1230	0.0033	0.1240	0.0060
384	0.1118	0.0032	0.1123	0.0029	0.1121	0.0052	0.1108	0.0044
511	0.0879	0.0026	0.0874	0.0024	0.0879	0.0040	0.0881	0.0042
662	0.0726	0.0021	0.0736	0.0019	0.0748	0.0031	0.0726	0.0029
835	0.0652	0.0025	0.0635	0.0021	0.0644	0.0027	0.0640	0.0031
1173	0.0513	0.0015	0.0523	0.0014	0.0517	0.0022	0.0519	0.0025
1275	0.0491	0.0014	0.0500	0.0012	0.0501	0.0021	0.0498	0.0021
1333	0.0478	0.0011	0.0480	0.0011	0.0486	0.0022	0.0492	0.0018

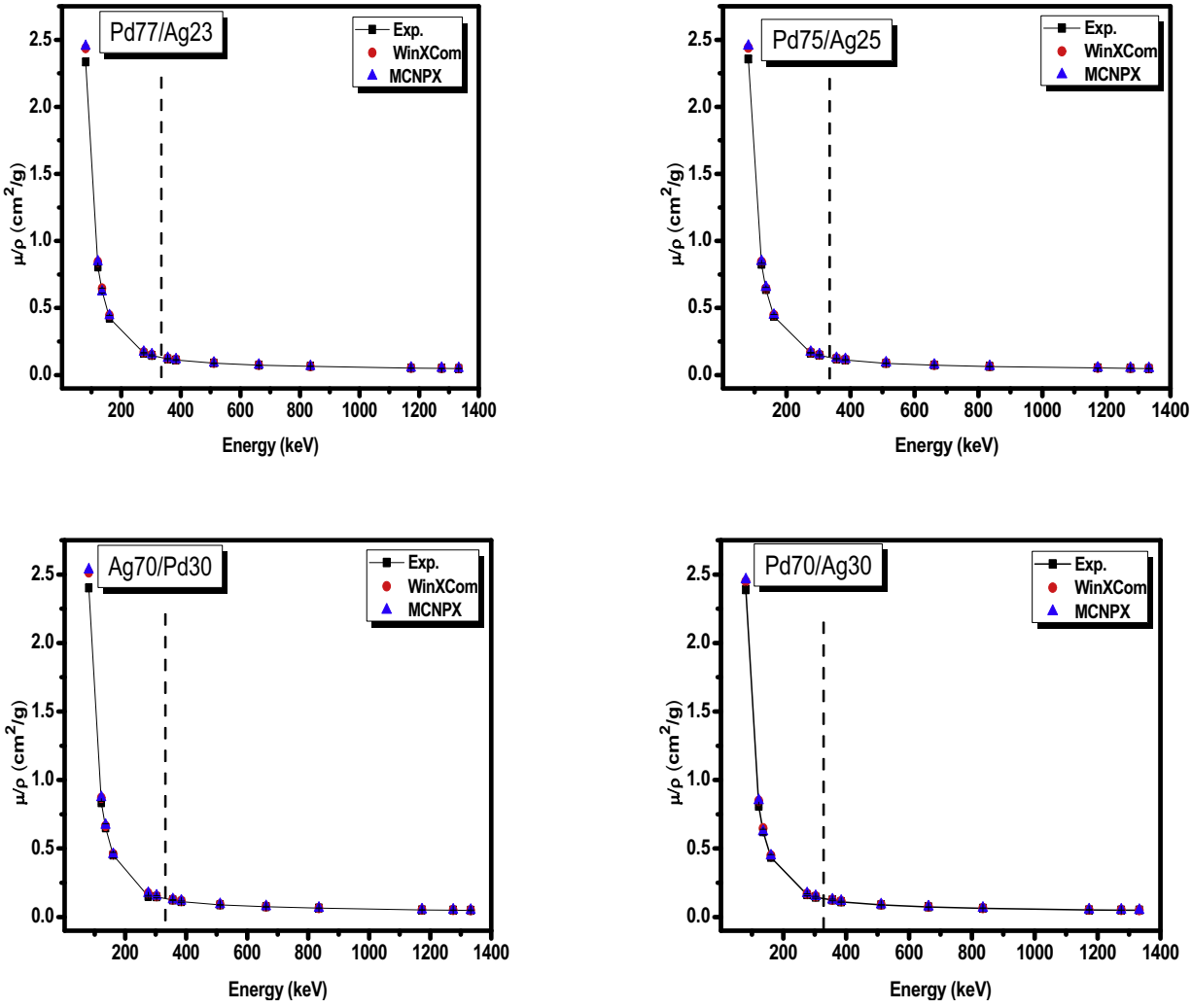

Fig. 3. Comparison of the experimental, WinXCom and MCNPX mass attenuation coefficients of different alloy samples.

Pd75/Ag25 demonstrated the highest gamma photon attenuation properties especially for the photon with low energy when compared to the other alloys. It is worth mention that Pd75/Ag25 has the highest density among the selected alloys and therefore, we can conclude that the density of the sample plays a decisive role in determining the number of gamma photons being attenuated when passing through the alloy sample. Pd75/Ag25 is denser than the rest of alloys (since the density of Pd and Ag is 12.023 g/cm^3 and 10.49 g/cm^3 respectively), thus more gamma photons being attenuated by this denser alloy sample, because the probability of the photons interaction with the atoms of the alloy sample is comparatively high due to tightly packed particle inside the

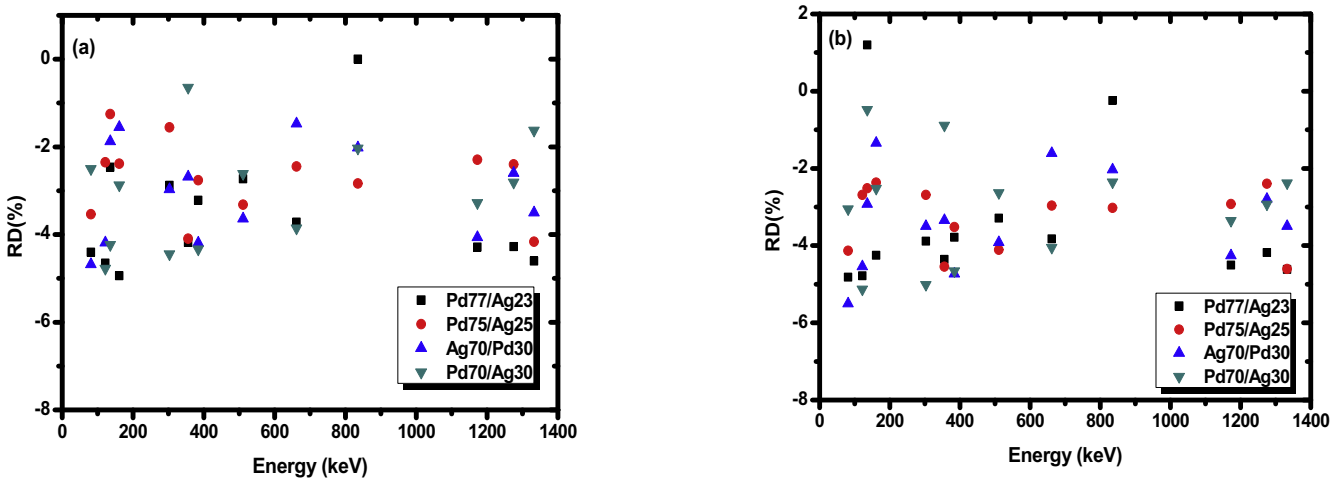

Fig. 4. The relative difference (RD) of (a) experimental–WinXCom results and (b) experimental– MCNPX results.

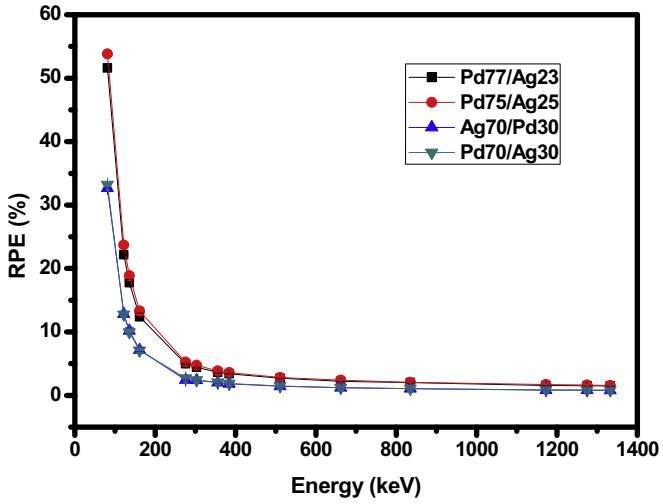

Fig. 5. The RPE values of the investigated alloys.

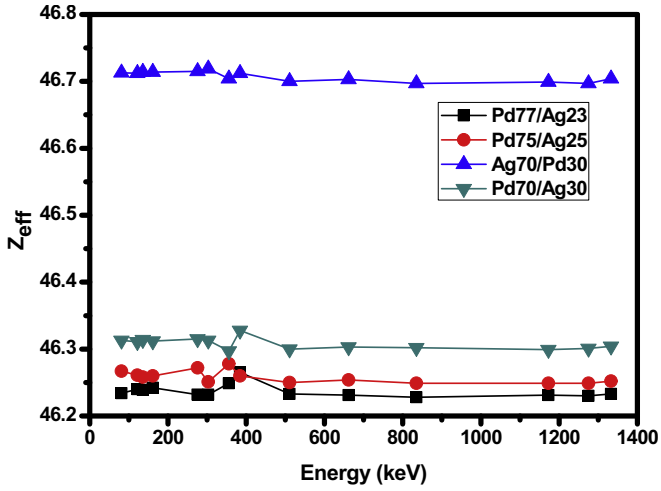

Fig. 6. The variation of effective atomic numbers depending on the energy for various alloys.

sample. This reveals that high-density alloy sample is more efficient than the lower density sample for attenuating the intensity of the incident gamma radiation.

The Z_{eff} values of these alloys that are composed of two elements with Z of 46 and 47, in different proportions have been calculated. Fig. 6 represents the obtained results at several energies from 81 keV to 1333 keV, which shows that the variation in Z_{eff} remains more or less stationary for all alloys expect for fluctuation at about 400 keV. It is found that the Z_{eff} values are related to the relative proportion of Z of elements of which the sample is composed and therefore increase with an increase in the Ag (Z = 47) concentrations as indicated in Fig. 6. The ranges of Z_{eff} are 46.228–46.242, 46.249–46.272, 46.299–46.315 and 46.697–46.719 for Pd77/Ag23, Pd75/Ag25, Pd70/Ag30 and Ag70/Pd30, respectively. The slight increase in Z_{eff} is attributed to the replacement of Pd content by Ag. El-Kateb et al. [38] reported similar results where Z_{eff} is almost constant for several samples such as steel, bronze, lead-antimony and aluminum-silicon.

The HVL values of the alloy samples under study have been calculated using the obtained μ values with help of Equation (8), and the values are plotted in Fig. 7(a). The range of HVL of the studied alloys is observed to be 0.03–1.21 cm, 0.03–1.23 cm, 0.023–1.30 cm and 0.025–1.31 cm for Pd70/Ag30, Pd75/Ag25, Pd77/Ag23 and Ag70/Pd30, respectively. As seen in Fig. 7(a), the lowest and highest HVL values are found for Pd75/Ag25 and Ag70/Pd30 alloy samples, respectively. The low HVL values of Pd75/Ag25 sample are based on the high density of this sample (ρ = 11.7 g/cm^3). This confirms that the gamma photon attenuation by the present alloys at different energies is extremely dependent on the density of the sample. The alloy of higher density provide a higher chances for the gamma photons to strike the atoms and this increases the probability of the photon interaction with these atoms and as a results a relatively few photons can transmitted from the alloy sample.

On other hand, it is highly required comparison of the photon shielding characteristic with previously reported various alloys to estimate the performance of the selected alloy samples and the probability of improvement as a alternative shielding material. The obtained HVL values of the investigated alloy samples are compared to those of Pd60/Cu40, Pd94/Cr6, Ag92.5/Cu7.5, and Ag72/Cu28 alloys published by Akman et al. [9]. While the HVL results of Ag70/Pd30 and Pd70/Ag30 samples are a rather similar as those of Ag92.5/Cu7.5, Pd60/Cu40 and Ag72/Cu28 alloys, the Pd75/Ag25 and Pd94/Cr6 sample has lowest and highest HVL values than results of the alloys under investigation. It is deduced from Fig. 7(b)

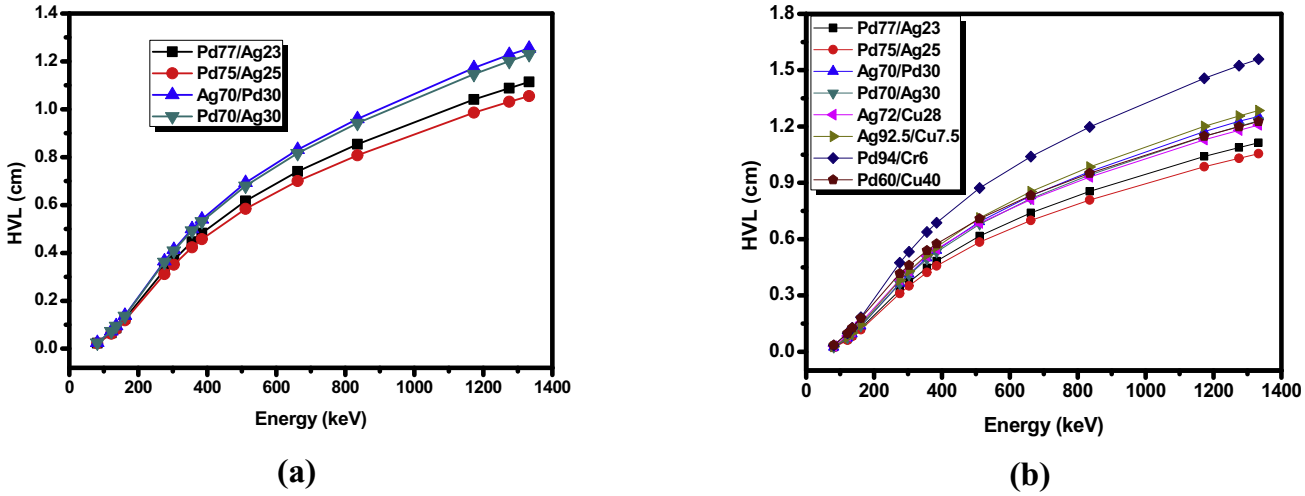

Fig. 7. Comparison of half value layers (HVLs) of (a) the studied alloys with (b) previous reported alloys [9].

that among the compared alloys, the Pd75/Ag25 sample will exhibit superior gamma ray shielding features in case of use as gamma radiation shielding material for any energy.

4. Conclusion

We reported μ/ρ, RPE, Z_{eff} and HVL for four alloy samples composed of different rates of Pd and Ag. The radiation shielding performances have been determined experimentally, theoretical (WinXCom software) and computational (MCNPX simulation code) at various energies from 81 to 1333 keV. The relative deviations between both experimental data-WinXCom and experimental data-MCNPX values are less than 6% which confirmed that the μ/ρ values were obtained with high accuracy. The reported results indicated that among the selected alloys, Pd75/Ag25 alloy sample has superior photon shielding characteristics. Moreover, the obtained data from this work can pioneer in points of development of new materials used as shielding materials. The presented radiation attenuation values of the investigated are extremely important for many fields such as medical applications, shielding researchers and radiation physics.

References

[1] S. Kaur, A. Kaur, P.S. Singh, T. Singh, Scope of Pb-Sn binary alloys as gamma rays shielding material, Prog. Nucl. Energy (2016), https://doi.org/10.1016/j.pnucene.2016.08.022.
[2] H. Singh, J. Sharma, T. Singh, Extensive investigations of photon interaction properties for ZnxTe100-x alloys, Nucl. Eng. Technol. 50 (2018) 1364–1371, https://doi.org/10.1016/j.net.2018.08.001.
[3] T. Kaur, J. Sharma, T. Singh, Thickness optimization of Sn–Pb alloys for experimentally measuring mass attenuation coefficients, Nucl. Energy Technol. 3 (2017) 1–5, https://doi.org/10.1016/j.nucet.2017.02.001.
[4] B. Aygün, E. Şakar, T. Korkut, M.I. Sayyed, A. Karabulut, M.H.M. Zaid, Fabrication of Ni, Cr, W reinforced new high alloyed stainless steels for radiation shielding applications, Results Phys (2019), https://doi.org/10.1016/j.rinp.2018.11.038.
[5] A.E. Ersundu, M. Büyükyıldız, M. Çelikbilek Ersundu, E. Şakar, M. Kurudirek, The heavy metal oxide glasses within the WO3-MoO3-TeO2system to investigate the shielding properties of radiation applications, Prog. Nucl. Energy (2018), https://doi.org/10.1016/j.pnucene.2017.10.008.
[6] D.K. Gaikwad, M.I. Sayyed, S.S. Obaid, S.A.M. Issa, P.P. Pawar, Gamma ray shielding properties of TeO2-ZnF2-As2O3-Sm2O3glasses, J. Alloy. Comp. 765 (2018) 451–458, https://doi.org/10.1016/j.jallcom.2018.06.240.
[7] D.K. Gaikwad, S.S. Obaid, M.I. Sayyed, R.R. Bhosale, V.V. Awasarmol, A. Kumar, M.D. Shirsat, P.P. Pawar, Comparative study of gamma ray shielding competence of WO3-TeO2-PbO glass system to different glasses and concretes, Mater. Chem. Phys. 213 (2018) 508–517, https://doi.org/10.1016/j.matchemphys.2018.04.019.
[8] S.S. Obaid, M.I. Sayyed, D.K. Gaikwad, P.P. Pawar, Attenuation coefficients and exposure buildup factor of some rocks for gamma ray shielding applications, Radiat. Phys. Chem. (2018), https://doi.org/10.1016/j.radphyschem.2018.02.026.
[9] F. Akman, M.I. Sayyed, M.R. Kaçal, H.O. Tekin, Investigation of photon shielding performances of some selected alloys by experimental data, theoretical and MCNPX code in the energy range of 81 keV–1333 keV, J. Alloy. Comp. (2019), https://doi.org/10.1016/j.jallcom.2018.09.177.
[10] V.P. Singh, N.M. Badiger, Study of mass attenuation coefficients, effective atomic numbers and electron densities of carbon steel and stainless steels, Radioprotection 48 (2013) 431–443, https://doi.org/10.1051/radiopro/2013067.
[11] I. Akkurt, Effective atomic numbers for Fe-Mn alloy using transmission experiment, Chin. Phys. Lett. 24 (2007) 2812–2814, https://doi.org/10.1088/0256-307X/24/10/027.
[12] I. Han, L. Demir, Determination of mass attenuation coefficients, effective atomic and electron numbers for Cr, Fe and Ni alloys at different energies, Nucl. Instrum. Methods Phys. Res. Sect. B Beam Interact. Mater. Atoms (2009), https://doi.org/10.1016/j.nimb.2008.10.004.
[13] O. Ielli, S. Erzeneoğlu, I.H. Karahan, G. Çankaya, Effective atomic numbers for CoCuNi alloys using transmission experiments, J. Quant. Spectrosc. Radiat. Transf. 91 (2005) 485–491, https://doi.org/10.1016/j.jqsrt.2004.07.006.
[14] J. Singh, H. Singh, J. Sharma, T. Singh, P.S. Singh, Fusible alloys: a potential candidate for gamma rays shield design, Prog. Nucl. Energy 106 (2018) 387–395, https://doi.org/10.1016/j.pnucene.2018.04.002.
[15] V.P. Singh, N.M. Badiger, Gamma ray and neutron shielding properties of some alloy materials, Ann. Nucl. Energy (2014), https://doi.org/10.1016/j.anucene.2013.10.003.
[16] X. Chen, L. Liu, F. Pan, J. Mao, X. Xu, T. Yan, Microstructure, electromagnetic shielding effectiveness andmechanical properties of Mg–Zn–Cu–Zr alloys, Mater. Sci. Eng. B Solid-State Mater. Adv. Technol. 197 (2015) 67–74, https://doi.org/10.1016/j.mseb.2015.03.012.
[17] H.C. Manjunatha, L. Seenappa, C. B.M, K.N. Sridhar, C. Hanumantharayappa, Gamma, X-ray and neutron shielding parameters for the Al-based glassy alloys, Appl. Radiat. Isot. (2018), https://doi.org/10.1016/j.apradiso.2018.05.014.
[18] L. Joska, M. Marek, J. Leitner, The mechanism of corrosion of palladium-silver binary alloys in artificial saliva, Biomaterials (2005), https://doi.org/10.1016/j.biomaterials.2004.05.018.
[19] J.H. Hubbell, Photon mass attenuation and energy-absorption coefficients, Int. J. Appl. Radiat. Isot. (1982), https://doi.org/10.1016/0020-708X(82)90248-4.
[20] L. Gerward, N. Guilbert, K.B. Jensen, H. Levring, WinXCom - a program for calculating X-ray attenuation coefficients, Radiat. Phys. Chem. (2004), https://doi.org/10.1016/j.radphyschem.2004.04.040.
[21] F. Akman, I.H. Geçibesler, I. Demirkol, A. Çetin, Determination of effective atomic numbers and electron densities for some synthesized triazoles from the measured total mass attenuation coefficients at different energies, Can. J. Phys. (2018). https://doi.org/10.1139/cjp-2017-0923 (in press).
[22] F. Akman, R. Durak, M.F. Turhan, M.R. Kaçal, Studies on effective atomic numbers, electron densities from mass attenuation coefficients near the K edge in some samarium compounds, Appl. Radiat. Isot. (2015), https://doi.org/10.1016/j.apradiso.2015.04.001.
[23] M.I. Sayyed, S.A.M. Issa, M. Büyükyıldız, M. Dong, Determination of nuclear radiation shielding properties of some tellurite glasses using MCNP5 code, Radiat. Phys. Chem. (2018), https://doi.org/10.1016/j.radphyschem.2018.04.014.
[24] F. Akman, M.R. Kaçal, F. Akman, M.S. Soylu, Determination of effective atomic numbers and electron densities from mass attenuation coefficients for some selected complexes containing lanthanides, Can. J. Phys. (2017), https://

doi.org/10.1139/cjp-2016-0811.
[25] T. Singh, A. Kaur, J. Sharma, P.S. Singh, Gamma rays' shielding parameters for some Pb-Cu binary alloys, Eng. Sci. Technol. an Int. J. (2018), https://doi.org/10.1016/j.jestch.2018.06.012.
[26] A. Kumar, Gamma ray shielding properties of PbO-Li2O-B2O3glasses, Radiat. Phys. Chem. 136 (2017) 50–53, https://doi.org/10.1016/j.radphyschem.2017.03.023.
[27] O. Agar, H.O. Tekin, M.I. Sayyed, M.E. Korkmaz, O. Culfa, C. Ertugay, Experimental investigation of photon attenuation behaviors for concretes including natural perlite mineral, Results Phys 12 (2019) 237–243, https://doi.org/10.1016/j.rinp.2018.11.053.
[28] O. Agar, Study on gamma ray shielding performance of concretes doped with natural sepiolite mineral, Radiochim. Acta 106 (2018) 1009–1016, https://doi.org/10.1515/ract-2018-2981.
[29] Maestro, No Title, Www.Ortec-Online.Com/Download/Maest. (2018).
[30] O. Agar, I. Boztosun, C. Segebade, Multielemental analysis of some soils in Karaman by PAA using a cLINAC, Appl. Radiat. Isot. 122 (2017) 57–62, https://doi.org/10.1016/j.apradiso.2017.01.011.
[31] F. Akman, I.H. Geçibesler, M.I. Sayyed, S.A. Tijani, A.R. Tufekci, I. Demirtas, Determination of some useful radiation interaction parameters for waste foods, Nucl. Eng. Technol. (2018), https://doi.org/10.1016/j.net.2018.05.007.
[32] H.S. Mann, G.S. Brar, K.S. Mann, G.S. Mudahar, Experimental investigation of clay fly ash bricks for gamma-ray shielding, Nucl. Eng. Technol. 48 (2016) 1230–1236, https://doi.org/10.1016/j.net.2016.04.001.
[33] M.I. Sayyed, F. Akman, I.H. Geçibesler, H.O. Tekin, Measurement of mass attenuation coefficients, effective atomic numbers, and electron densities for different parts of medicinal aromatic plants in low-energy region, Nucl. Sci. Tech. 29 (2018), https://doi.org/10.1007/s41365-018-0475-0.
[34] O. Agar, Z.Y. Khattari, M.I. Sayyed, H.O. Tekin, S. Al-Omari, M. Maghrabi, M.H.M. Zaid, I.V. Kityk, Evaluation of the shielding parameters of alkaline earth based phosphate glasses using MCNPX code, Results Phys 12 (2019) 101–106, https://doi.org/10.1016/j.rinp.2018.11.054.
[35] M.I. Sayyed, M.G. Dong, H.O. Tekin, G. Lakshminarayana, M.A. Mahdi, Comparative investigations of gamma and neutron radiation shielding parameters for different borate and tellurite glass systems using WinXCom program and MCNPX code, Mater. Chem. Phys. 215 (2018) 183–202, https://doi.org/10.1016/j.matchemphys.2018.04.106.
[36] O. Agar, M.I. Sayyed, H.O. Tekin, K.M. Kaky, S.O. Baki, I. Kityk, An investigation on shielding properties of BaO , MoO 3 and P 2 O 5 based glasses using MCNPX code, Results Phys 12 (2019) 629–634, https://doi.org/10.1016/j.rinp.2018.12.003.
[37] S.A.M. Issa, Y.B. Saddeek, H.O. Tekin, M.I. Sayyed, K. saber Shaaban, Investigations of radiation shielding using Monte Carlo method and elastic properties of PbO-SiO2-B2O3-Na2O glasses, Curr. Appl. Phys. (2018), https://doi.org/10.1016/j.cap.2018.02.018.
[38] A.H. El-Kateb, R.A.M. Rizk, A.M. Abdul-Kader, Determination of atomic cross-sections and effective atomic numbers for some alloys, Ann. Nucl. Energy (2000), https://doi.org/10.1016/S0306-4549(99)00121-8.